

Investigating the selectivity of calcium hypochlorite for flotation separation of chalcopyrite and pyrite pre-adsorbed collector

Wenhui Yang ¹, Xianhui Qiu ^{1,2}, Huashan Yan ^{1,2}, Hao Wu ¹, Liu Yang ¹, Ruisen Lai ¹, Tingsheng Qiu ^{1,2}

¹ School of Resource and Environment Engineering, Jiangxi University of Science and Technology, Ganzhou 341000, China

² Jiangxi Province Key Laboratory of Mining Engineering, Jiangxi University of Science and Technology, Ganzhou 341000, China

Corresponding authors: qiuxianhui@126.com (X. Qiu), qitingsheng@163.com (T. Qiu)

Abstract: Bulk flotation is usually used in the flotation of Cu-Fe sulfide ore, and the subsequent concentrate is difficult to be separated because the minerals have adsorbed the collector. In this paper, flotation tests showed that calcium hypochlorite ($\text{Ca}(\text{ClO})_2$) had a stronger depression effect on pyrite pre-adsorbed sodium butyl xanthate (SBX), while having a negligible depressive effect on chalcopyrite. A copper concentrate with Cu grade of 33.32% and Cu recovery of 94.47% could be obtained from flotation tests of mixed minerals. The depression performance and mechanism of $\text{Ca}(\text{ClO})_2$ were studied by contact angle measurements, Fourier transform infrared spectroscopy and X-ray photoelectron spectroscopy analyses, the results suggested that $\text{Ca}(\text{ClO})_2$ can decompose SBX on the pyrite surface and oxidizes the mineral surface to form hydrophilic substances, which enhances the hydrophilicity of the pyrite surface. In contrast, $\text{Ca}(\text{ClO})_2$ has little effect on chalcopyrite pre-adsorbed SBX, the possible depression model is discussed.

Keywords: pyrite, chalcopyrite, calcium hypochlorite, flotation separation

1. Introduction

Copper is mostly extracted from chalcopyrite (Li et al., 2013). However, chalcopyrite is usually associated with other sulfide ores, especially pyrite; froth flotation is a common method for separating sulphide ores, but it cannot easily separate chalcopyrite and pyrite because they have similar floatability (Chen et al., 2021; Sarquís et al., 2014). The existence of pyrite not only dilutes the grade of chalcopyrite concentrate but also has a great impact on the subsequent metallurgical process, as pyrite produces sulfur dioxide (SO_2) in the smelting process and pollutes the environment (Forbes et al., 2018; Khoso et al., 2019). Therefore, the separation of chalcopyrite from pyrite has always been difficult, and the problem of separation needs to be solved urgently. Lime and cyanide have been commonly used as pyrite depressants for decades. However, lime not only depresses pyrite under strong alkaline conditions, which causes environmental pollution and pipeline blockage, but also causes low recovery of precious metals, such as gold and silver, and it is difficult to activate pyrite in subsequent recovery. Cyanide is highly toxic and will cause great harm to people and the environment. Certain organic depressants, such as starch, guar gum, dextrin and carboxymethyl cellulose, are inexpensive and easy to obtain, but their large dosage and poor selectivity limit their use (Li et al., 2021; Liu et al., 2020; Shen et al., 2021). Therefore, it is of great significance to explore agents with a strong depression effect on pyrite and little effect on chalcopyrite.

As a strong oxidant, calcium hypochlorite ($\text{Ca}(\text{ClO})_2$) is widely used in the bleaching of pulp in the papermaking industry and cotton, linen and other fabrics in the textile industry. It is also used to sterilise and disinfect urban and rural drinking water and swimming pool water. In addition, $\text{Ca}(\text{ClO})_2$ is used in the chemical industry for the purification of acetylene and the manufacture of chloroform and other organic chemical raw materials (Yigit et al., 2009). It is also gradually being used

in the mineral processing flotation separation of sulfide minerals. Yin et al. (2019) used $\text{Ca}(\text{ClO})_2$ to selectively separate pyrite and covellite. Pyrite was preferentially oxidised by $\text{Ca}(\text{ClO})_2$, forming CaSO_4 and $\text{Fe}(\text{OH})_3$ on its surface. Therefore, the adsorption of the collector on the surface of pyrite was prevented, leading to the depression of pyrite. $\text{Ca}(\text{ClO})_2$ strongly depressed pyrite while having almost no effect on covellite, and it separated the two sulfide minerals. Liu et al. (2015) selectively separated galena and jamesonite with $\text{Ca}(\text{ClO})_2$. $\text{Ca}(\text{ClO})_2$ produced high concentrations of OH^- and $\text{Ca}(\text{OH})^+$, which competed with the collectors in being adsorbed on the surface of jamesonite. $\text{Ca}(\text{ClO})_2$ strongly depressed jamesonite and slightly depressed galena, thus completing the separation of the two minerals. Therefore, $\text{Ca}(\text{ClO})_2$ can be used as a depressant for the selective separation of sulfide minerals.

In the flotation process of Cu-Fe sulphide ores, the bulk flotation is often adopted, chalcopyrite and pyrite mixed concentrate is obtained by adding a collector, such as sodium butyl xanthate (SBX). The collector is adsorbed on the minerals surface, which makes the subsequent flotation separation more difficult. There are only a few studies on this type of separation depressant for chalcopyrite and pyrite mixed concentrate. In this paper, flotation tests indicate that $\text{Ca}(\text{ClO})_2$ had a stronger depression effect on pyrite pre-adsorbed sodium butyl xanthate (SBX), while having a negligible depressive effect on chalcopyrite. The selective depressant mechanism of $\text{Ca}(\text{ClO})_2$ on SBX-adsorbed pyrite was studied by contact angle measurements, Fourier transform infrared (FTIR) spectroscopy and X-ray photoelectron spectroscopy (XPS).

2. Materials and methods

2.1. Materials and reagents

The chalcopyrite and pyrite used in the tests are high-purity natural minerals obtained from Hubei Province in China. After careful manual selection, they were crushed and ground into suitably sized particles with a hammer and a porcelain ball mill. Chalcopyrite and pyrite are transformed into particles sized -0.074 mm to $+0.038$ mm for flotation tests. The chemical compositions of the chalcopyrite and pyrite samples were determined by chemical composition analyses, the results, shown in Table 1 and X-ray diffraction (XRD) Fig. 1 show that the purity of chalcopyrite and pyrite is more than 95%.

Table 1. Main chemical compositions of chalcopyrite and pyrite (wt%)

Components	Fe	S	Cu	Purity
Chalcopyrite	30.41	35.11	33.15	95.31 %
Pyrite	44.92	52.00	-	96.25 %

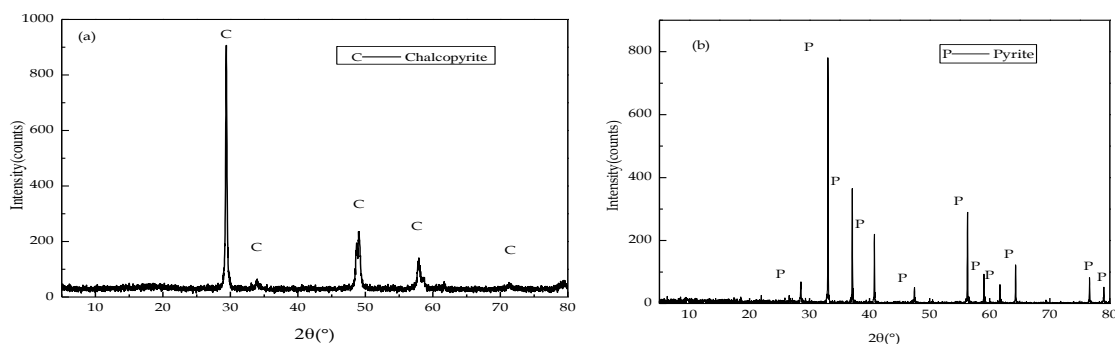


Fig. 1. XRD patterns of samples: (a) chalcopyrite, (b) pyrite

The collector (SBX), frother (methyl isobutyl carbinol [MIBC]), depressant ($\text{Ca}(\text{ClO})_2$), pH regulator (sodium hydroxide [NaOH]) and hydrochloric acid (HCl) used in this experiment were of analytical grade. Potassium bromide (KBr) of spectroscopic grade used in FTIR spectroscopy measurements was supplied by Tianjin Hengchuang Lida Technology Development Co., Ltd. The water used in the whole experiment was deionized (DI) water.

2.2. Micro-flotation tests

Micro-flotation tests were conducted in an XFG₁₁₅₀ laboratory flotation machine with a stirring speed of 1992 r/min. First, 2 g of the mineral samples was added to 40 mL DI water, and the minerals are introduced into the flotation cell for flotation. Then, the collector (SBX), pH regulator, depressant ($\text{Ca}(\text{ClO})_2$) and frother (MIBC) are added at intervals of 3 min, 3 min and 1 min, respectively. After flotation for 4 min, the obtained concentrate products and tailings were placed in glass dishes and weighed after being dried in a laboratory oven. A flowchart of the micro-flotation tests is shown in Fig. 2. The recovery of chalcopyrite and pyrite is based on the weight of the dried concentrate products and tailings.

Mixed-mineral flotation tests are performed to verify the selective separation of chalcopyrite and pyrite by $\text{Ca}(\text{ClO})_2$. The mass ratio of chalcopyrite to pyrite is 1:1, and the process is the same as that of the micro-flotation tests. The recovery rate of chalcopyrite was calculated according to copper grade. The flotation tests were performed in triplicate, the average values are reported. Moreover, the standard deviation was calculated and reported as error bar.

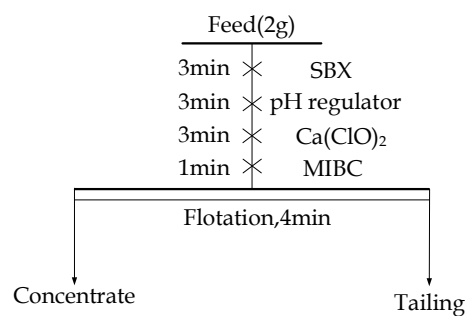


Fig. 2. Flowchart of flotation tests

2.3. Contact angle measurements

In this study, the contact angles between chalcopyrite and pyrite before and after reagent treatment are measured in a JY-82C contact angle meter. Before the test, one side of the massive chalcopyrite and pyrite was polished to expose the fresh surface, and then the mineral samples were treated with flotation reagents, and the dosing sequence is consistent with that in the micro-flotation test. The treated samples were dried in a vacuum oven at 40 °C, and the mineral contact angle was measured. Each test was repeated three times, and the average is reported as the final result in this study.

2.4. FTIR analyses

FTIR was used to measure the reagents and mineral samples before and after reagent treatment. The test samples were ground to $-5\ \mu\text{m}$, and reagent was added. The addition method and sequence of the reagents were consistent with those in the micro-flotation test. After the reagents interacted with the minerals, the test samples were filtered and washed three times with deionised water. The samples were then dried in a vacuum oven at a temperature of 40 °C. Finally, the prepared sample was mixed with spectral-grade KBr at a mass ratio of 1:100, loaded into a mold and pressed for FTIR measurement. The resolution and scanning range of the spectrum are $4\ \text{cm}^{-1}$ and $400\text{--}4000\ \text{cm}^{-1}$, respectively, and there are 32 scans.

2.5. XPS analyses

XPS was used to determine and analyse differences in the chemical compositions and chemical states of the elements on the surface of chalcopyrite and pyrite before and after reagent treatment. The preparation process of the sample is consistent with that in the flotation process. After fully interacting with the reagent, the mineral sample was washed with DI water three times, dried in a vacuum oven at a temperature of 40 °C and subjected to XPS assessment. Before analysis, all binding energies of the XPS spectra were corrected with the standard adsorption peak of C1s (284.8 eV) data (Xie et al., 2020).

3. Results and discussion

3.1. Single mineral flotation tests

Fig. 3 (a) shows the relationship between SBX concentration and flotation recovery of chalcopyrite and pyrite when the pulp pH is about 7. With increasing of SBX concentration, the recovery of chalcopyrite and pyrite gradually increases. When the concentration of SBX increases to 20 mg/L, the recovery of chalcopyrite reaches 96% and then gradually levels off with a further increase in the SBX concentration. Fig. 3 (b) reflects the relationship between pH and the flotation recovery of chalcopyrite and pyrite when the SBX concentration is 20 mg/L. When the xanthate concentration is determined, the recovery of chalcopyrite is always above 94% and that of pyrite is above 90% with changes of pH. The change in pH has little effect on the flotation recovery of chalcopyrite and pyrite.

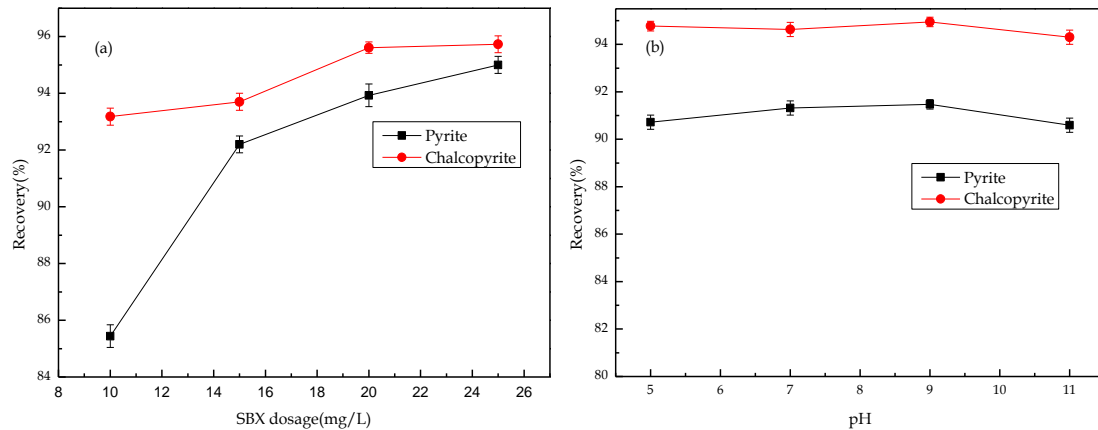


Fig. 3. (a) Effect of SBX dosage on the flotation behaviour of chalcopyrite and pyrite, (b) Effect of pH on the flotation behaviour of chalcopyrite and pyrite at SBX dosage of 20 mg/L

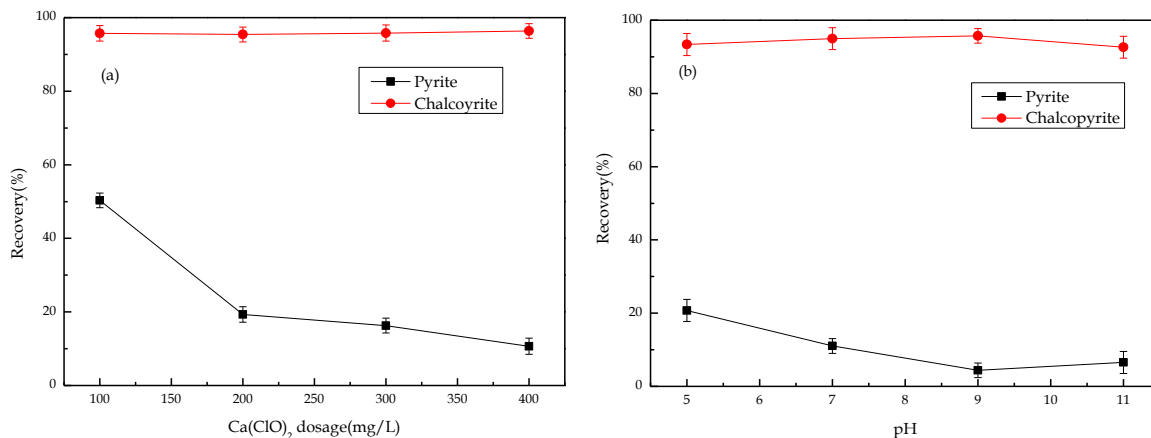


Fig. 4. (a) Effect of $\text{Ca}(\text{ClO})_2$ dosage on flotation behaviour of chalcopyrite and pyrite at pH of about 7, (b) Effect of pH on flotation behaviour of chalcopyrite and pyrite at $\text{Ca}(\text{ClO})_2$ dosage of 200 mg/L

The relationship between $\text{Ca}(\text{ClO})_2$ concentration and the flotation recovery of chalcopyrite and pyrite are shown in Fig. 4 (a). When the pulp pH is about 7, the increase in $\text{Ca}(\text{ClO})_2$ concentration has little effect on the flotation recovery of chalcopyrite. Even when the concentration reaches the maximum value of 400 mg/L, the recovery of chalcopyrite remains over 90%. In contrary, when the concentration of $\text{Ca}(\text{ClO})_2$ exceeds 200 mg/L, the recovery of pyrite decreases to less than 20%. The above results show that $\text{Ca}(\text{ClO})_2$ has a much greater depression effect on SBX-adsorbed pyrite than on chalcopyrite with increasing concentration.

The pH condition tests were conducted when the concentration of $\text{Ca}(\text{ClO})_2$ was 200 mg/L, the relationship between the pH change and the flotation recovery of chalcopyrite and pyrite can be seen in Fig. 4(b). The pH change has no evident effect on the flotation recovery of chalcopyrite. In the whole

pH range, the flotation recovery of chalcopyrite remains above 90%. In contrary, when the concentration of $\text{Ca}(\text{ClO})_2$ was 200 mg/L, the flotation recovery of pyrite was less than 25% in the whole pH range. When the pH is 9–11, the flotation recovery of pyrite is less than 10%.

3.2. Mixed-mineral flotation tests

Two groups of tests (with and without $\text{Ca}(\text{ClO})_2$) are compared to investigate the selective depression effect of $\text{Ca}(\text{ClO})_2$ on the mixed minerals of chalcopyrite and pyrite. The results are presented in Table 2. The mixed-mineral flotation tests were performed at an SBX concentration of 20 mg/L, and the pH was adjusted to approximately 10. The Cu grades in the concentrates and tailings are 33.32% and 1.46%, respectively, and the recovery of Cu in the concentrates is 94.47%. The concentrate yield without $\text{Ca}(\text{ClO})_2$ is 95.31%, and the grade of copper in the concentrates is only 17.02%. The flotation test results show that $\text{Ca}(\text{ClO})_2$ can significantly depress pyrite adsorbed with SBX but has no significant effect on chalcopyrite adsorbed with SBX. Therefore, the addition of $\text{Ca}(\text{ClO})_2$ enhances the depression of pyrite in chalcopyrite–pyrite flotation separation.

Table 2. Flotation separation results of chalcopyrite–pyrite mixed minerals

	Products	Mass	Copper	Copper
		recovery	grade (%)	recovery (%)
		(Wt./%)	Cu	Cu
Without $\text{Ca}(\text{ClO})_2$	Concentrate	95.31	17.02	97.90
	Tailing	4.69	7.42	2.10
With $\text{Ca}(\text{ClO})_2$	Concentrate	42.79	33.32	94.47
	Tailing	57.21	1.46	5.53

3.3. Contact angle measurements

The relationship between the contact angle of the chalcopyrite and pyrite surface and the change in the $\text{Ca}(\text{ClO})_2$ concentration are shown in Fig. 5. Without the addition of $\text{Ca}(\text{ClO})_2$, the contact angles of chalcopyrite and pyrite with SBX adsorbed as the collector are 97° and 84° respectively. After $\text{Ca}(\text{ClO})_2$ treatment of chalcopyrite and pyrite adsorbed with SBX, the contact angle of chalcopyrite decreased slightly and finally decreased to approximately 90° . However, with the increase of $\text{Ca}(\text{ClO})_2$ concentration, the contact angle of pyrite decreased to 55° , indicating that the surface hydrophobicity of pyrite decreases more obviously than that of chalcopyrite. When the $\text{Ca}(\text{ClO})_2$ concentration exceeds 100 mg/L, the contact angle of the two minerals significantly differs in a manner that is conducive to the separation of chalcopyrite and pyrite.

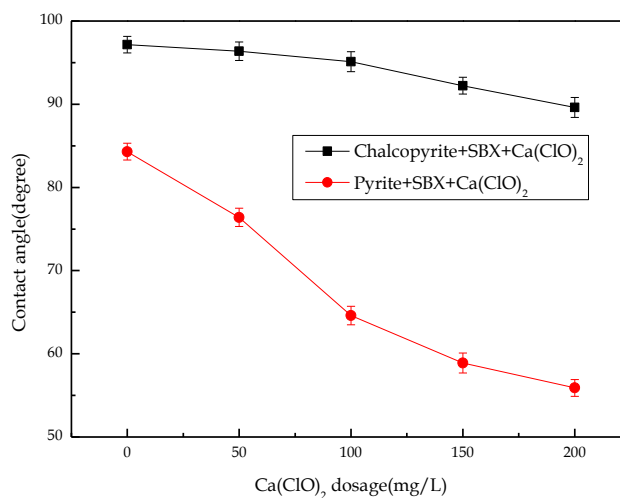


Fig. 5. Effect of $\text{Ca}(\text{ClO})_2$ dosage on chalcopyrite and pyrite surface contact angle

3.4. FTIR analysis

Infrared spectroscopy was performed to clarify the adsorption mechanism between the flotation reagents and mineral surfaces. As shown in Fig. 6, in the spectrum of SBX, the peaks detected at 2870 cm^{-1} and 2960 cm^{-1} are the vibration peaks of $-\text{CH}_2$ and $-\text{CH}_3$, respectively, and the peak at 1445 cm^{-1} is the stretching vibration peak of $-\text{C}(\text{S})\text{S}$. The main absorption peak of xanthate is the stretching vibration of $\text{C}-\text{O}-\text{C}$, $\text{C}=\text{S}$ and $\text{C}-\text{S}$ from 1074 cm^{-1} to 1152 cm^{-1} (Wang et al., 2021; Wei et al., 2021).

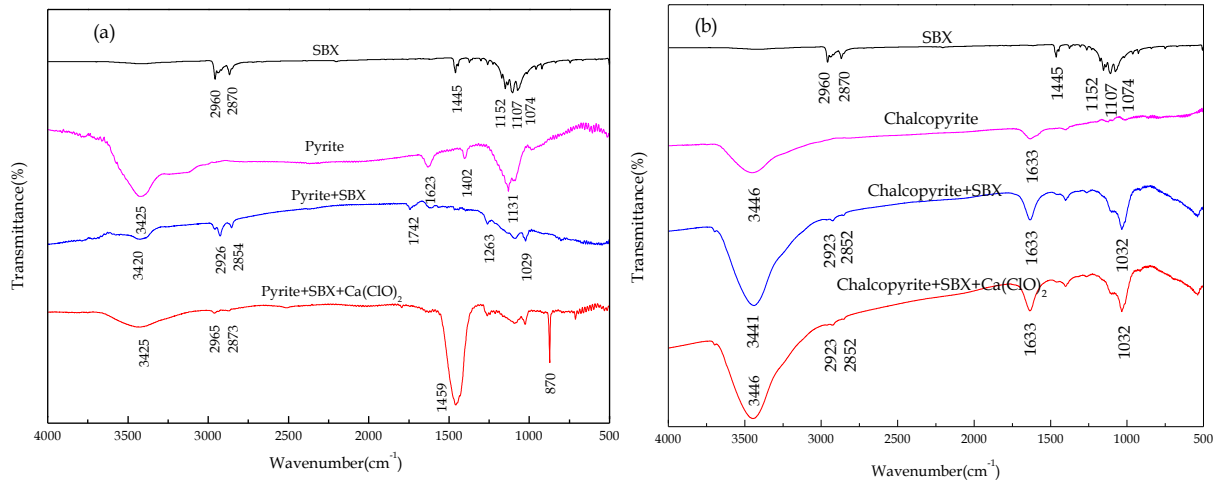


Fig. 6. (a) Infrared Spectra of pyrite before and after $\text{Ca}(\text{ClO})_2$ treatment, (b) chalcopyrite before and after $\text{Ca}(\text{ClO})_2$ treatment

As clearly depicted in Fig. 6 (a), the peaks at 1623 cm^{-1} , 1402 cm^{-1} and 1131 cm^{-1} are characteristic of pyrite (Zhang et al., 2021). In the spectra after SBX treatment, new peaks appear in the spectrogram, namely, $-\text{CH}_2$ (2854 cm^{-1}) and $-\text{CH}_3$ (2926 cm^{-1}), due to the movement of the xanthate characteristic peaks $-\text{CH}_2$ (2870 cm^{-1}) and $-\text{CH}_3$ (2960 cm^{-1}), respectively. The characteristic peaks of pyrite shift significantly, indicating that xanthate induces chemisorption on the surface of pyrite. After pyrite interacts with SBX and then with $\text{Ca}(\text{ClO})_2$, the characteristic peaks $-\text{CH}_3$ (2926 cm^{-1}) and $-\text{CH}_2$ (2854 cm^{-1}) shift significantly to $-\text{CH}_3$ (2965 cm^{-1}) and $-\text{CH}_2$ (2873 cm^{-1}), respectively, and the intensity of the adsorption peak decreases significantly. A characteristic peak of $\text{Ca}(\text{ClO})_2$ appears and shifts significantly from 1417 cm^{-1} to 1459 cm^{-1} .

The spectra of chalcopyrite and chalcopyrite after reagent treatment are displayed in Fig. 6 (b). In the spectra after SBX treatment, new peaks appear in the spectrum, namely, $-\text{CH}_3$ (2923 cm^{-1}) and $-\text{CH}_2$ (2852 cm^{-1}), due to the shift of the characteristic peaks $-\text{CH}_2$ (2870 cm^{-1}) and $-\text{CH}_3$ (2960 cm^{-1}) of xanthate, respectively. As the xanthate absorption peak $\text{C}=\text{S}$ (1074 cm^{-1}) moves, a new peak appears, namely, $\text{C}=\text{S}$ (1032 cm^{-1}). After $\text{Ca}(\text{ClO})_2$ treatment, the characteristic peaks $-\text{CH}_3$ (2923 cm^{-1}) and $-\text{CH}_2$ (2852 cm^{-1}) and the absorption peak $\text{C}=\text{S}$ (1032 cm^{-1}) do not shift. These results show that $\text{Ca}(\text{ClO})_2$ causes chemisorption on the surface of pyrite adsorbed xanthate, but has no obvious effect on the surface of chalcopyrite adsorbed xanthate.

3.5. XPS analysis

Previous tests and analyses proved that $\text{Ca}(\text{ClO})_2$ is chemically adsorbed on pyrite with adsorbed SBX. The chemical states of the products generated on the mineral surface can be more clearly reflected by XPS (Gao et al., 2018; Zhang et al., 2021). XPS tests were performed on chalcopyrite and pyrite before and after reagent treatment to further explore the depression mechanism of $\text{Ca}(\text{ClO})_2$ on pyrite with adsorbed SBX. The obtained XPS spectra are shown in Figs. 7 and 8.

The high-resolution spectra of $\text{Fe}2\text{p}$ and $\text{S}2\text{p}$ of pyrite before and after reagent treatment are displayed in Fig. 7. As shown in Fig. 7(a), the peak at 707.32 eV is the fully coordinated low-spin Fe^{2+} site in pyrite, and the peak at 707.97 eV is the $\text{Fe}(\text{II})-\text{S}$ multistate splitting peak (Graham and Bower, 2012). After pyrite is treated with SBX, a new peak appears at a binding energy of 709.00 eV, which is the $\text{Fe}(\text{II})-\text{S}$ bond in $\text{Fe}-\text{SBX}$. After treatment with $\text{Ca}(\text{ClO})_2$, the peak of xanthate disappears, and the

peaks observed at the higher binding energies of 711.01 eV and 712.41 eV are the multistate splitting peaks of Fe³⁺ oxygen or hydroxyl compounds (Fe(II)-O/OH) (Boulton et al., 2003; Kalegowda et al., 2015; Niu et al., 2019). As presented in Fig. 7(b), the peak at 161.91 eV is monosulfide (S²⁻) on the pyrite surface, the peak at 162.81 eV is disulfide (S₂²⁻), and the peak at 165.08 eV is attributed to polysulphide and elemental sulphur (Sn²⁻/S⁰) (Han et al., 2019; Mu et al., 2017). After pyrite is treated with SBX, a new peak appears at 163.80 eV due to the S-C bond of SBX adsorption. After Ca(ClO)₂ treatment, the xanthate peaks disappear, and oxidation peaks of SO₄²⁻ (Fe₂(SO₄)₃ and FeSO₄) are observed at the higher binding energies of 168.10 eV and 169.90 eV (Mikhlin et al., 2016; Niu et al., 2019). This indicates that Ca(ClO)₂ decomposes the SBX adsorbed on the surface of pyrite and oxidizes the surface of pyrite to produce hydrophilic substances.

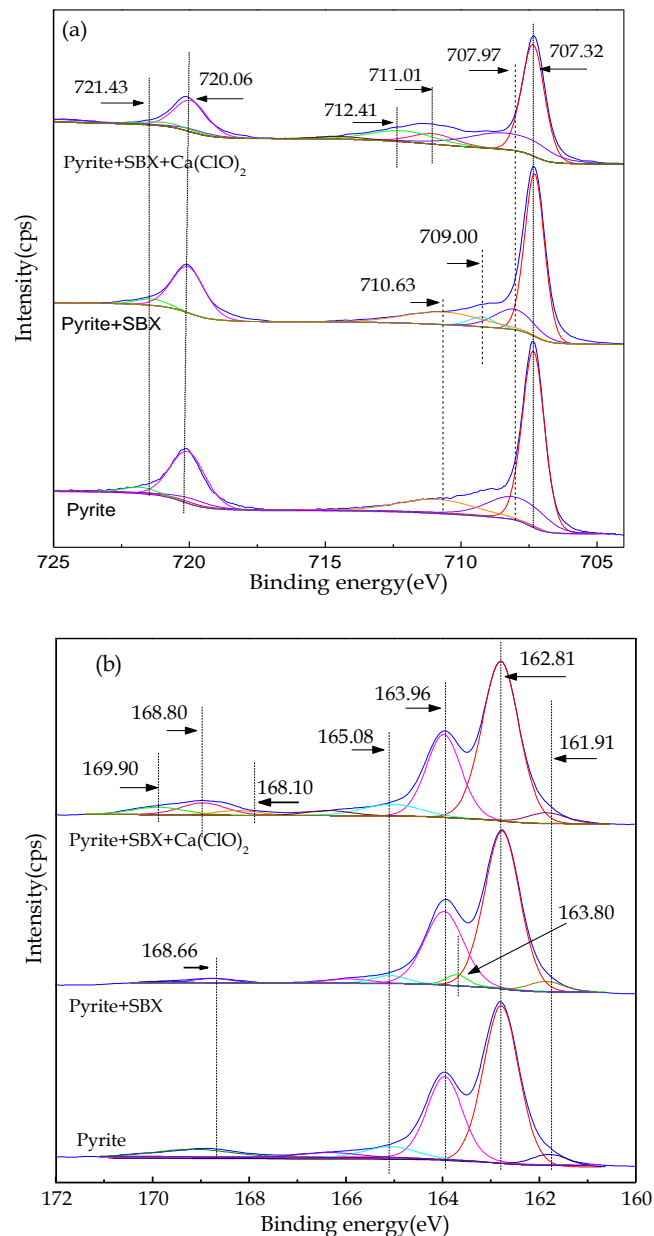


Fig. 7. (a) High-resolution spectra of Fe2p of pyrite before and after reagent treatment, (b) High-resolution spectra of S2p of pyrite before and after reagent treatment

Fig. 8 illustrates the high-resolution spectra of Cu2p, Fe2p and S2p of chalcopyrite before and after chemical treatment. As shown in Fig. 8(a), all peaks in the spectrum of Cu2p of chalcopyrite shift after xanthate treatment, and the peak at 933.63 eV is the Cu-S bond in Cu-SBX (Huang et al., 2019). The spectrum of Cu2p of chalcopyrite treated with Ca(ClO)₂ is almost the same as that of Cu2p treated

with SBX. As shown in Fig. 8(b), after chalcopyrite is treated with SBX, some characteristic separation peaks of chalcopyrite in the Fe2p spectrum of chalcopyrite are shifted, and the peak at 721.54 eV is the Fe-S bond in Fe-SBX (Wang et al., 2021). The spectrum of Fe2p of chalcopyrite treated with $\text{Ca}(\text{ClO})_2$ is almost the same as that of Fe2p treated with SBX. It can be seen in Fig. 8(c), after chalcopyrite is treated with SBX, all peaks in the S2p spectrum of chalcopyrite are shifted, and the peak at 161.50 eV is the S-C bond in xanthate (Kalegowda et al., 2015). The spectrum of S2p of chalcopyrite treated with $\text{Ca}(\text{ClO})_2$ is almost the same as that of S2p treated with SBX. This shows that $\text{Ca}(\text{ClO})_2$ has little effect on the surface of chalcopyrite adsorbed with xanthate.

Based on the above analyses, a possible depression mechanism diagram showing how $\text{Ca}(\text{ClO})_2$ depresses pyrite with pre-adsorbed collector SBX is proposed, as shown in Fig. 9. In the flotation process, $\text{Ca}(\text{ClO})_2$ decomposes the SBX adsorbed on the surface of pyrite and oxidizes the mineral surface, thus generating hydrophilic substances that result in the hydrophilicity of the pyrite surface. In contrast, $\text{Ca}(\text{ClO})_2$ has no significant effect on the SBX adsorbed on the surface of chalcopyrite, and chalcopyrite floats hydrophobically. Therefore, $\text{Ca}(\text{ClO})_2$ can be used as an effective depressant of chalcopyrite-pyrite with an adsorbed collector.

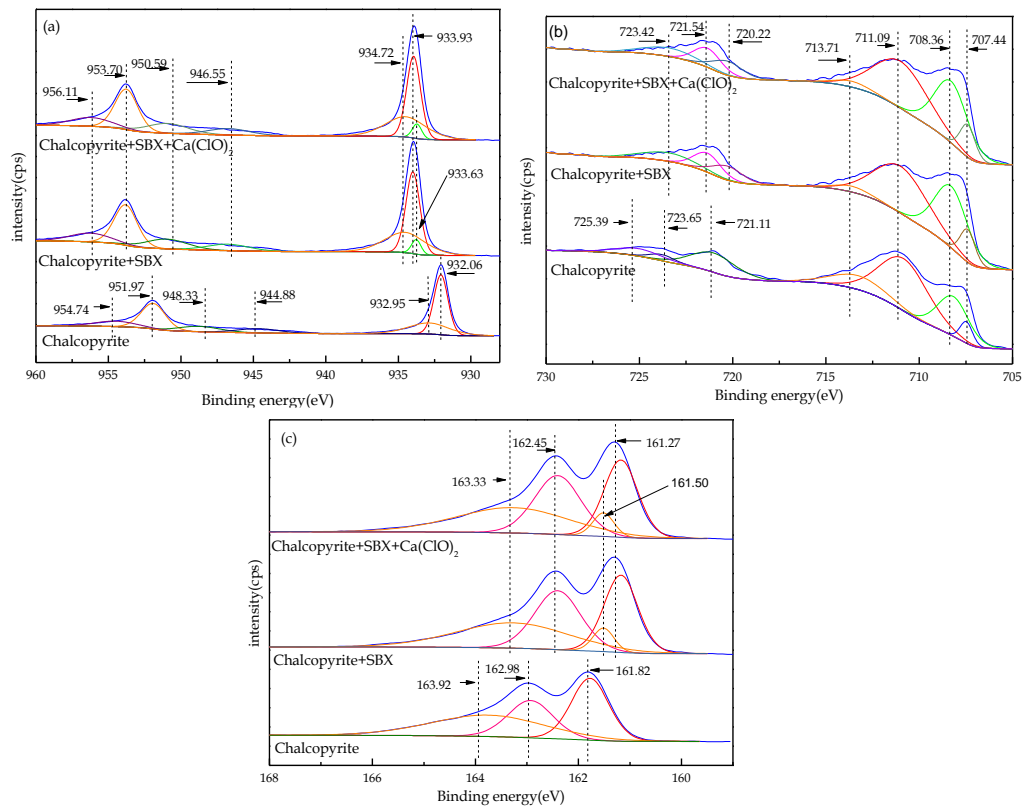


Fig. 8. (a) High-resolution spectra of Cu2p of chalcopyrite before and after reagent treatment, (b) Cu2p of chalcopyrite Fe2p, (c) S2p of chalcopyrite

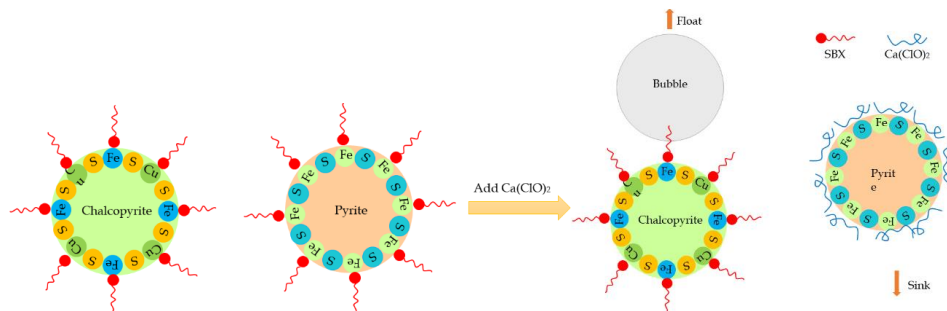


Fig. 9. Possible depression model for selective separation of chalcopyrite-pyrite adsorbed with SBX by $\text{Ca}(\text{ClO})_2$

4. Conclusions

In this paper, $\text{Ca}(\text{ClO})_2$ is used as a depressant for the selective separation of chalcopyrite and pyrite with pre-adsorbed collector SBX. Single mineral flotation tests and mixed-mineral flotation tests showed that $\text{Ca}(\text{ClO})_2$ can obviously depress pyrite but induces little depression on chalcopyrite. Contact angle measurement results show that, even if xanthate is adsorbed, $\text{Ca}(\text{ClO})_2$ can significantly enhance the hydrophilicity of the pyrite surface, whereas chalcopyrite treated with $\text{Ca}(\text{ClO})_2$ maintains strong hydrophobicity. FTIR and XPS analysis results suggested that when $\text{Ca}(\text{ClO})_2$ is used to treat chalcopyrite and pyrite with pre-adsorbed SBX, the xanthate adsorbed on the surface of pyrite is decomposed, and the mineral surface is oxidized, hydrophilic substance formed on pyrite surface, while the surface of chalcopyrite is almost unchanged. The results of this study provide insights into the depression mechanism of $\text{Ca}(\text{ClO})_2$ on pyrite with adsorbed xanthate, and this method offers reference value for studies on the flotation separation of chalcopyrite–pyrite mixed concentrates with adsorbed collectors.

Acknowledgments

This work was supported by the National Key R&D Program of China (2018YFC1902002), the National Natural Science Foundation of China (No. 51974138) and The Program of Qingjiang Excellent Young Talents (JXUSTQJYX2020021), Jiangxi University of Science and Technology.

References

- BOULTON, A., FORNASIERO, D., RALSTON, J., 2003. *Characterisation of sphalerite and pyrite flotation samples by xps and tof-sims*. International Journal of Mineral Processing, 70, 205-219.
- CHEN, J., WANG, J., LI, Y., LIU, M., LIU, Y., ZHAO, C., CUI, W., 2021. *Effects of surface spatial structures and electronic properties of chalcopyrite and pyrite on z-200 selectivity*. Minerals Engineering, 163, 106803.
- FORBES, E., SMITH, L., VEPSALAINEN, M., 2018. *Effect of pyrite type on the electrochemistry of chalcopyrite/pyrite interactions*. Physicochemical Problems of Mineral Processing, 54.
- GAO, Y., GAO, Z., SUN, W., YIN, Z., WANG, J., HU, Y., 2018. *Adsorption of a novel reagent scheme on scheelite and calcite causing an effective flotation separation*. Journal of Colloid and Interface Science, 512, 39-46.
- GRAHAM, A.M., BOUWER, E.J., 2012. *Oxidative dissolution of pyrite surfaces by hexavalent chromium: surface site saturation and surface renewal*. Geochimica et Cosmochimica Acta, 83, 379-396.
- HAN, G., WEN, S., WANG, H., FENG, Q., 2019. *Lactic acid as selective depressant for flotation separation of chalcopyrite from pyrite and its depression mechanism*. Journal of Molecular Liquids, 296, 111774.
- HUANG, X., HUANG, K., JIA, Y., WANG, S., CAO, Z., ZHONG, H., 2019. *Investigating the selectivity of a xanthate derivative for the flotation separation of chalcopyrite from pyrite*. Chemical Engineering Science, 205, 220-229.
- KALEGOWDA, Y., CHAN, Y., WEI, D., HARMER, S.L., 2015. *X-peem, xps and tof-sims characterisation of xanthate induced chalcopyrite flotation: effect of pulp potential*. Surface Science, 635, 70-77.
- KHOSO, S.A., HU, Y., LYU, F., LIU, R., SUN, W., 2019. *Selective separation of chalcopyrite from pyrite with a novel non-hazardous biodegradable depressant*. Journal of Cleaner Production, 232, 888-897.
- LI, M., LIAN, D., ZHAO, F., TONG, X., WU, C., GAO, X., 2021. *Structure-activity of chelating depressants for chalcopyrite/pyrite separation: dft study and flotation experiment*. Physicochemical Problems of Mineral Processing.
- LI, Y., KAWASHIMA, N., LI, J., CHANDRA, A.P., GERSON, A.R., 2013. *A review of the structure, and fundamental mechanisms and kinetics of the leaching of chalcopyrite*. Advances in Colloid and Interface Science, 197-198, 1-32.
- LIU, D., ZHANG, G., CHEN, Y., HUANG, G., GAO, Y., 2020. *Investigations on the utilization of konjac glucomannan in the flotation separation of chalcopyrite from pyrite*. Minerals Engineering, 145, 106098.
- LIU, R., GUO, Y., WANG, L., SUN, W., TAO, H., HU, Y., 2015. *Effect of calcium hypochlorite on the flotation separation of galena and jamesonite in high-alkali systems*. Minerals engineering, 84, 8-14.
- MIKHLIN, Y., KARACHAROV, A., TOMASHEVICH, Y., SHCHUKAREV, A., 2016. *Cryogenic xps study of fast-frozen sulfide minerals: flotation-related adsorption of n-butyl xanthate and beyond*. Journal of Electron Spectroscopy and Related Phenomena, 206, 65-73.
- MU, Y., LI, L., PENG, Y., 2017. *Surface properties of fractured and polished pyrite in relation to flotation*. Minerals Engineering, 101, 10-19.
- NIU, X., CHEN, J., LI, Y., XIA, L., LI, L., SUN, H., RUAN, R., 2019. *Correlation of surface oxidation with xanthate*

- adsorption and pyrite flotation. Applied Surface Science*, 495, 143411.
- SARQUÍS, P.E., MENÉNDEZ-AGUADO, J.M., MAHAMUD, M.M., DZIOBA, R., 2014. *Tannins: the organic depressants alternative in selective flotation of sulfides. Journal of cleaner production*, 84, 723-726.
- SHEN, Z., WEN, S., HAN, G., ZHOU, Y., BAI, X., FENG, Q., 2021. *Selective depression mechanism of locust bean gum in the flotation separation of chalcopyrite from pyrite in a low-alkalinity media. Minerals Engineering*, 170, 107044.
- WANG, X., LIU, J., ZHU, Y., HAN, Y., 2021. *Adsorption and depression mechanism of an eco-friendly depressant pca onto chalcopyrite and pyrite for the efficiency flotation separation. Colloids and Surfaces A: Physicochemical and Engineering Aspects*, 620, 126574.
- WEI, Q., DONG, L., JIAO, F., QIN, W., PAN, Z., CUI, Y., 2021. *The synergistic depression of lime and sodium humate on the flotation separation of sphalerite from pyrite. Minerals Engineering*, 163, 106779.
- XIE, R., ZHU, Y., LIU, J., WANG, X., & LI, Y., 2020. *Differential collecting performance of a new complex of decyloxy-propyl-amine and a-bromododecanoic acid on flotation of spodumene and feldspar. Minerals Engineering*, 153, 106377.
- YIGIT, O., SOYUNCU, S., ERAY, O., ENVER, S., 2009. *Inhalational and dermal injury due to explosion of calcium hypochlorite. Cutaneous and Ocular Toxicology*, 28, 37-40.
- YIN, W., YANG, B., FU, Y., CHU, F., YAO, J., CAO, S., ZHU, Z., 2019. *Effect of calcium hypochlorite on flotation separation of covellite and pyrite. Powder Technology*, 343, 578-585.
- ZHANG, Q., WEN, S., FENG, Q., LIU, Y., 2021. *Activation mechanism of lead ions in the flotation of sulfidized azurite with xanthate as collector. Minerals Engineering*, 163, 106809.